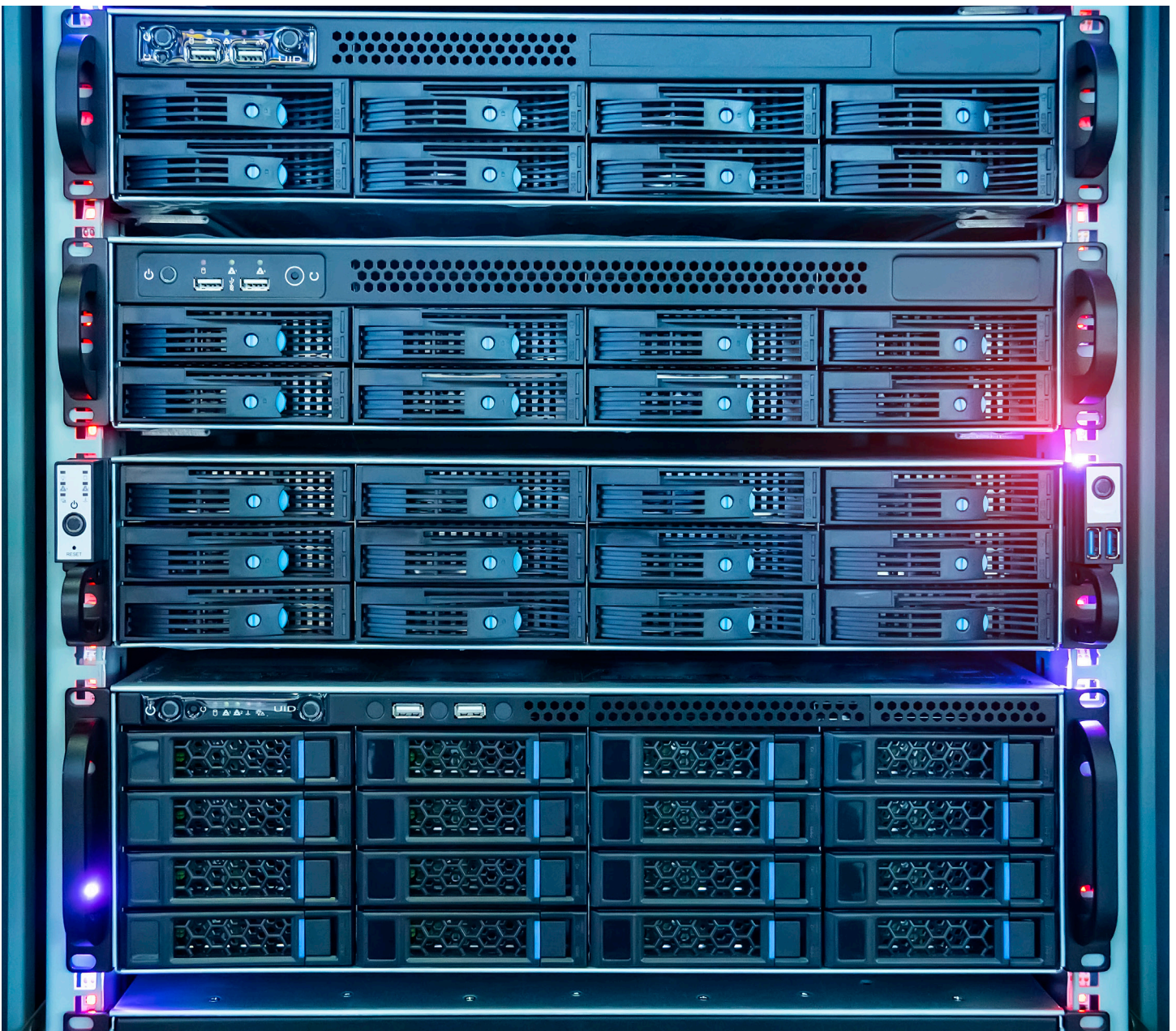


# Modeling Frequency Response of a Novel Pulse Width Modulated Flyback Control Scheme

Adrian Umadhay, Sean Zantua | Power Integrations, Philippines



## Abstract

This paper describes the controller design, small-signal modeling, and validation of a flyback power supply system based on an enhanced pulse width modulated (PWM) control technique capable of excellent output voltage regulation and very high efficiency across a wide range of line and load conditions. A math-based model was formulated to predict the frequency response of the flyback, compensation network, and controller – deriving the closed-loop frequency response of the power supply system across all modes of operation. The model correlates closely to measured system frequency response, precisely predicting the parameters of a stable, well-regulated, and efficient power supply.

## 1. Introduction

The regulatory landscape for power conversion continually raises requirements for efficiency for power supplies. In this paper we discuss a novel PWM control technique capable of excellent output voltage regulation and very high efficiency across a wide range of line and load conditions.

The flyback controller examined here regulates the switched-mode power supply's output voltage using a variable frequency and variable peak current control scheme. The approach can be used in both continuous conduction mode (CCM) and discontinuous conduction mode (DCM).

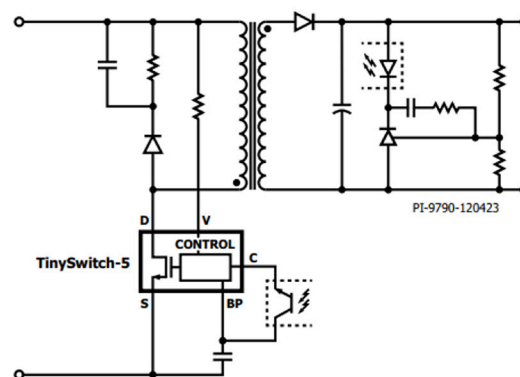
This addresses the evolving demands in the appliance and consumer market by enabling power supply solutions that deliver consistent performance across line and load conditions and meet regulatory requirements for no-load input power, standby, and light-load efficiencies while remaining cost effective – the control scheme allows a simplification of the power supply architecture and reduces part count.

The control loop employs a type II compensation network that provides the signal needed by the controller to regulate the flyback output voltage. This closed-loop system contains analog components in the control loop, so it is important to verify its time-domain stability.

This paper will focus on the small-signal modeling of the controller and its associated power supply architecture, as well as the verification of the model – which can be used to predict the frequency-domain response and time-domain stability of the system prior to physical prototyping [1].

## 2. Control Method

In a classical PWM-controlled flyback converter, the controller regulates the output voltage of the flyback converter by modulating the duty cycle of the primary-side power switch.



Basic power supply architecture

---

In this control scheme, the controller regulates the output voltage of the flyback converter by modulating the off-time and the magnetizing current limit for the primary-side switch, as opposed to just the duty cycle for the classical PWM control.

The power supply architecture associated with this PWM control scheme consists of a single-stage flyback converter, a type II compensation network with a shunt regulator, an optocoupler to cross the isolation barrier, and the controller.

The output voltage of the flyback converter is sampled using a feedback resistor network and converted to an optocoupler feedback current using the type II compensation network.

The optocoupler feedback current is converted by the off-time modulator to an off-time signal. The off-time is modulated inversely to the load – meaning the off-time increases as the output load decreases.

At the end of the off-time, the controller turns on the primary-side power switch which begins to ramp the primary magnetizing current. The current ramp is measured, and the switch is turned off when the current exceeds the limit set by the control engine (proportional to switching frequency).

The control engine's current limit threshold is controlled by the switching frequency. This characteristic produces a current limit that increases as the switching frequency increases.

As the load decreases, the switching frequency also decreases, resulting to a lower primary magnetizing current limit. The current limit can go as low as 30 percent of the maximum current limit threshold (determined by the switch size and maximum operating frequency).

Once the primary magnetizing current reaches the current limit set by the control engine, the primary-side power switch is turned off and the control is passed to the off-time modulator.

The combination of primary-side peak current and off-time modulation results in an improvement in light-load efficiency, standby efficiency, and no-load power consumption, which are critical for efficiency regulatory requirements.

### 3. Small-Signal Modeling

In steady state, the control loop regulates the output voltage of the flyback converter (plant) using a type II compensation network and the controller logic. The controller uses off-time modulation and peak current modulation to determine the off-time and on-time of the primary-side power switch of the flyback plant.

It is important to verify the time-domain stability of the PWM-controlled power supply because of the usage of analog components in its control loop, particularly in the compensation network. Selecting the correct component values ensures a stable closed-loop system response that can respond to perturbations in system inputs and outputs.

The conventional way to determine time-domain stability of a closed-loop power supply is by examining its frequency-domain response to see whether it complies with the classical bode stability criterion [1].

To predict the bode stability of the closed-loop system, a mathematical small-signal model was formulated. This section will describe the formulation and validation of the small-signal model for this closed-loop power supply system.

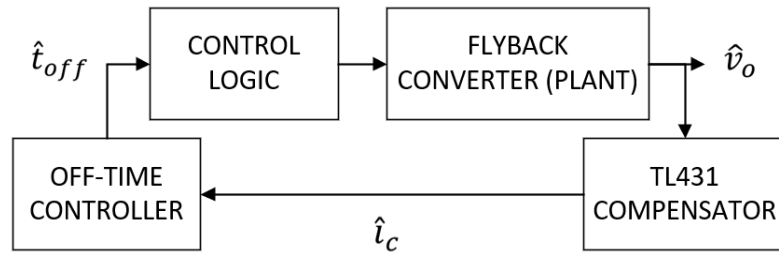


Fig. 1 High-level system block diagram

$$1) \frac{\hat{v}_o}{\hat{t}_{off}} \times \frac{\hat{i}_c}{\hat{v}_o} \times \frac{\hat{t}_{off}}{\hat{v}_c} = 1$$

$$2) \frac{\hat{v}_o}{\hat{t}_{off}} = \frac{G_{vd} \times F_t}{F_d \times G_{id} - G_{vd} \times F_v}$$

$$3) \frac{\hat{i}_c}{\hat{v}_o} = \frac{G_i \times \left(1 + \frac{Z_{type2}}{Z_{fbt}}\right)}{Z_{led} + R_{opto}}$$

$$4) \frac{\hat{t}_{off}}{\hat{i}_c} = \frac{(1-D)^2}{10.56 \times 10^{-12} \times f_{sw}^2}$$

The closed-loop power supply system was converted to a small-signal model representation. The small-signal model was then broken down into four blocks as shown in Fig. 1. The four blocks of the model are the flyback converter, the TL431 compensator, off-time controller, and finally the control logic.

The flyback converter and the control logic were combined and modelled together as a transfer function given by  $\hat{v}_o/\hat{t}_{off}$  or the small-signal output voltage over the small-signal off-time. This small-signal off-time to output-voltage transfer function, as shown in Eq. (1), works for both CCM and DCM operations without the need for separate equations.

The  $G_{vd}$  and  $G_{id}$  variables in the equation represent the duty-to-output voltage and duty-to-primary magnetizing current transfer functions, respectively. The  $F_t$ ,  $F_d$ , and  $F_v$  variables represent internal slopes and constants from the dynamics of the control logic with the flyback plant.

The dynamics of the control logic with the flyback plant lead to a control characteristic that does not distinguish between different conduction modes. This made it possible to create a singular-transfer function for the flyback plant and control logic that works for both CCM and DCM.

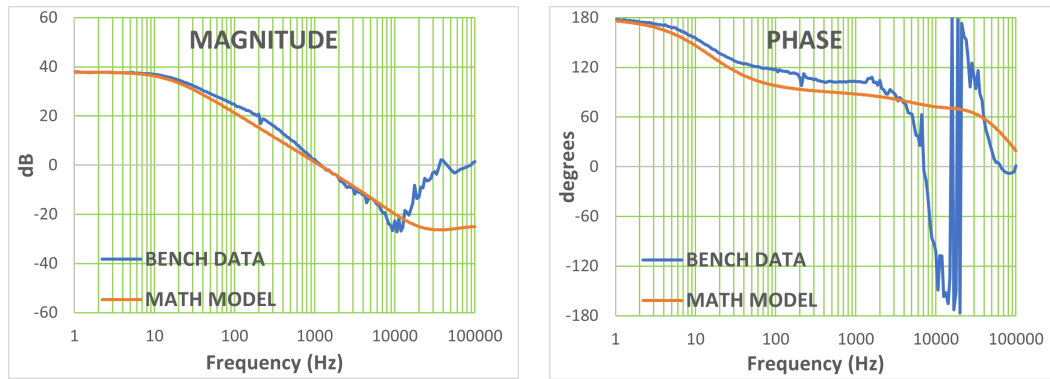


**Fig. 2 Math model vs. bench data correlation CCM Input: 110 VDC, Output: 24 V, 12.5 A**

The TL431 compensator block represents the complete compensation network composed of the feedback resistor network as the output voltage sensor, the type II compensation network using a TL431 shunt regulator, and the optocoupler. This block is modelled as a transfer function given by  $\hat{i}_c/\hat{v}_o$  or the small-signal control current over the small-signal output voltage, shown in Eq. (3). In this function,  $G_i$  is a gain, and  $Z_{type2}$ ,  $Z_{fbt}$ ,  $Z_{led}$ , and  $R_{opto}$  are impedance terms from the compensation network.

Finally, the off-time controller block is modeled as a transfer function given by  $\hat{t}_{off}/\hat{i}_c$  or the small-signal off-time over the small-signal control current, shown in Eq. (4). In this function,  $D$  represents duty cycle and  $f_{sw}$  represents the switching frequency. The product of these three transfer function ratios, in Eq. (1), represent the closed-loop small-signal model of the power supply system.

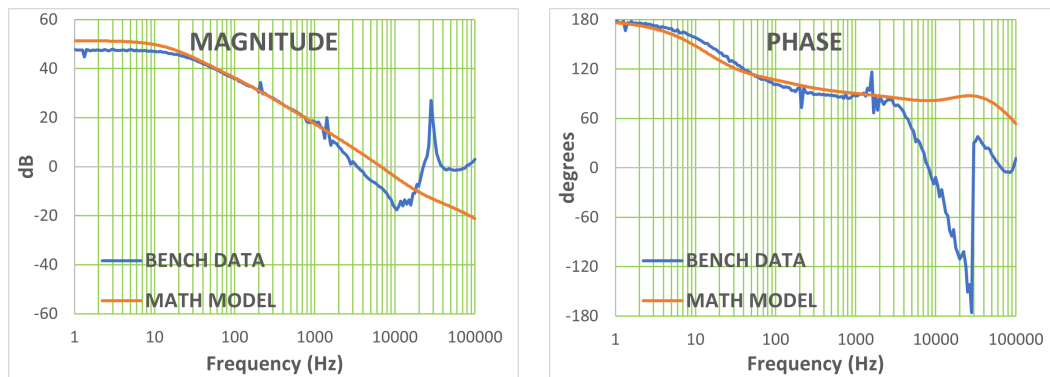


**Fig. 3 Math model vs. bench data correlation DCM Input: 310 VDC, Output: 24 V, 12.5 A**

The mathematical small-signal model of the closed-loop system was formulated in MATLAB and correlated with the actual control loop performance on the bench.

## 4. Performance Evaluation

The frequency response of a prototype 300 W (24 V, 12.5 A) flyback power supply using the described PWM control algorithm was evaluated in both CCM and DCM operation using a frequency response analyzer (FRA). The measured frequency response data from the 300 W power supply prototype was correlated with the mathematical small-signal model using the inputs and design parameters from the 300 W design.

While measuring the control loop response, a steady-state operating point was selected, with respect to which the frequency and current limit are time-invariant. A small-signal perturbation introduced to the output voltage will result in a variation in the off-time, peak current, and duty cycle determined by the controller. This, in turn, will result in variations in the output voltage of the flyback. The FRA can measure these variations in the output voltage and determine its magnitude and phase relative to the introduced perturbations.

The frequency response of the 300 W prototype was first measured in CCM condition, operating at 110 VDC input voltage, full-load output of 24 V, 12.5 A, and switching at 120 kHz frequency. As for the DCM condition, the frequency response of the prototype was measured at 310 VDC input, full load of 24 V, 12.5 A, and switching frequency of 108 kHz.

The frequency response or bode plots of the prototype are shown in Fig. 2 for the CCM condition and Fig. 3 for the DCM condition. Magnitude and phase are plotted separately. The blue plots are the data measured from bench FRA while the orange plots are the data from the mathematical small-signal model.

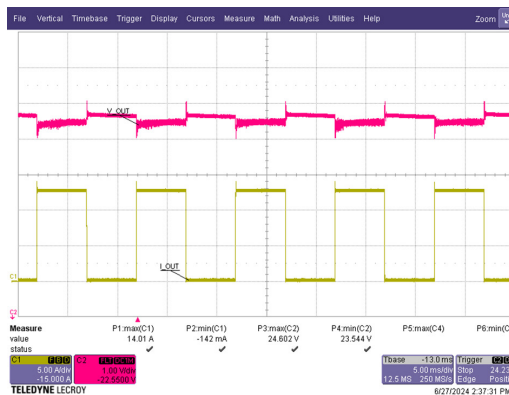


**Fig. 4 Load transient response; Input: 115 VAC, 60 Hz, Output: 24 V, 0 A – 12.5 A, 5 ms**

In CCM, the bench bode plot crosses over at 1.2 kHz, with a DC gain of 38 dB, and a phase margin more than 90 degrees. As for the DCM bench bode plot, the crossover frequency is around 3 kHz, the DC gain is 48 dB, and the phase margin is above 75 degrees.

The measured frequency response of the prototype power supply correlates closely to the frequency response predicted by the mathematical small-signal model, as shown in Fig. 2 and Fig. 3. The model can predict the shape of the magnitude and phase plots relatively closely, especially for the lower frequencies up to the crossover frequency.

The phase margin for both CCM and DCM is measured to be greater than 75 degrees indicating good stability. This also translates to excellent load transient response at 115 VAC and 230 VAC line input as illustrated in Fig. 4 and Fig. 5, respectively [2][3]. The load transient response plots were tested at 0 percent to 100 percent load at intervals of 5 ms. The output voltage exhibited a very fast settling time and minimal voltage overshoot of less than 3 percent, demonstrating the robustness of the design.

Accurate output voltage regulation across line and load conditions is shown in Fig. 6 and Fig. 7, exhibiting regulation less than 1 percent of the nominal output. This was made possible by the high DC gain exhibited in the bode plots from Fig. 2 and Fig. 3. The very high DC gain, which comes from the off-time modulation in Eq. (4), results in a negligible steady-state error, providing excellent output voltage regulation [1][3].

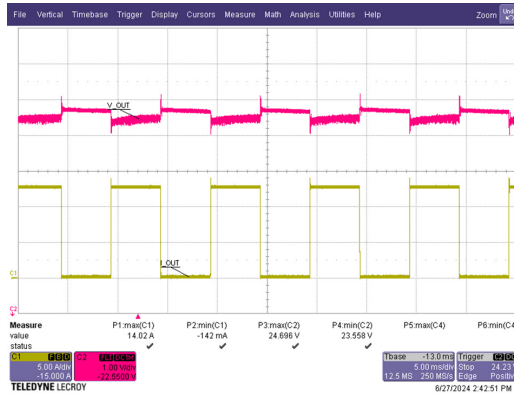


Fig. 5 Load transient response; Input: 230 VAC, 50 Hz, Output: 24 V, 0 A – 12.5 A, 5 ms

Figures 8 and 9 show the efficiency curves for the power supply across various line and load conditions. This demonstrates the advantage of the control engine in achieving high and flat efficiency across a wide range of line and load, making it easier for designers to comply with efficiency regulations.

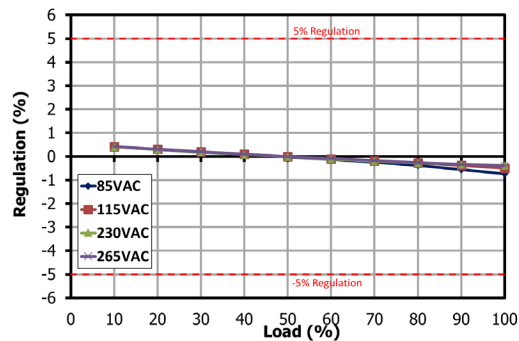


Fig. 6 Output voltage regulation vs. output load

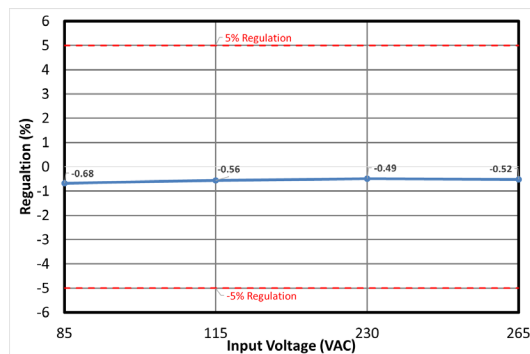


Fig. 7 Output voltage regulation vs. input line

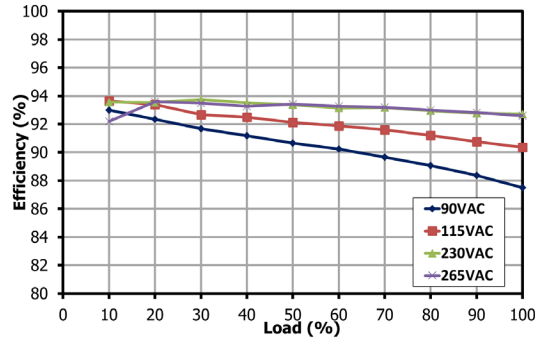


Fig. 8 Efficiency (%) across output load

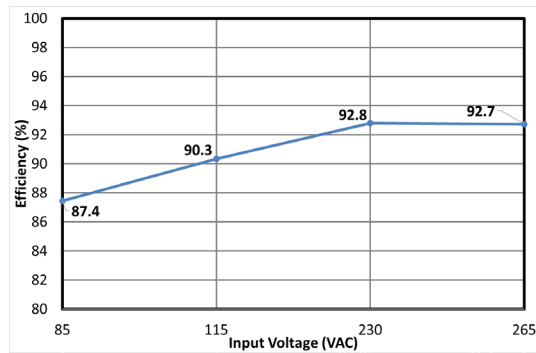


Fig. 9 Efficiency (%) across input line

## 5. Conclusion

A prototype power supply design utilizing the novel PWM control scheme described in this paper was built and tested to assess its stability and robustness. The mathematical small-signal model, which was developed to predict the frequency response of the system, yielded excellent correlation in both magnitude and phase with the bench data from the prototype. The novel approach used by the control engine allows designers to achieve high efficiency across different line and load conditions. The high DC gain provided by the off-time controller, coupled with the variable frequency of operation, resulted in excellent output voltage regulation and transient response, and avoids the problems caused by the bandwidth limitations encountered when using conventional optocouplers in the feedback loop.

## References

- [1] R. W. Erickson and D. Maksimović, “Fundamentals of Power Electronics, 2nd ed.” New York, NY, USA: Kluwer Academic, 2001.
- [2] C. Basso, “Switching Power Supply Design, 2nd ed.” New York, NY, USA: McGraw-Hill Education, 2008.
- [3] K. Ogata, “Modern Control Engineering, 5th ed.” Upper Saddle River, NJ, USA: Prentice Hall, 2010.

---

For more information,  
visit **power.com**<sup>™</sup>



© 2025 Power Integrations | Power Integrations, the Power Integrations logo, power.com, PowiGaN, and InnoSwitch are trademarks or registered trademarks of Power Integrations, Inc., in the U.S. and/or other countries.